

Kinetics and Mechanism of the Reaction of Chlorine Atoms with *n*-Pentanal

E. Iwasaki, T. Nakayama, and Y. Matsumi

Solar–Terrestrial Environment Laboratory and Graduate School of Science, Nagoya University,
Furo-cho, Chikusa, Nagoya 464-8601, Japan

K. Takahashi

Kyoto University Pioneering Research Unit For Next Generation, Kyoto University Gokasho,
Uji, Kyoto 611-0011, Japan

T. J. Wallington* and M. D. Hurley

Ford Motor Company, P.O. Box 2053, Dearborn, Michigan 48121-2053

E. W. Kaiser

Department of Natural Sciences, 4901 Evergreen Road, University of Michigan–Dearborn,
Dearborn, Michigan 48128

Received: September 18, 2007; In Final Form: November 30, 2007

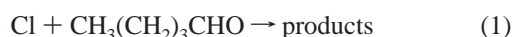
The kinetics and mechanism of the reaction $\text{Cl} + \text{CH}_3(\text{CH}_2)_3\text{CHO}$ was investigated using absolute (PLP–LIF) and relative rate techniques in 8 Torr of argon or 800–950 Torr of N_2 at 295 ± 2 K. The absolute rate experiments gave $k[\text{Cl} + \text{CH}_3(\text{CH}_2)_3\text{CHO}] = (2.31 \pm 0.35) \times 10^{-10}$ in 8 Torr of argon, while relative rate experiments gave $k[\text{Cl} + \text{CH}_3(\text{CH}_2)_3\text{CHO}] = (2.24 \pm 0.20) \times 10^{-10} \text{ cm}^3 \text{ molecule}^{-1} \text{ s}^{-1}$ in 800–950 Torr of N_2 . Additional relative rate experiments gave $k[\text{Cl} + \text{CH}_3(\text{CH}_2)_3\text{C}(\text{O})\text{Cl}] = (8.74 \pm 1.38) \times 10^{-11} \text{ cm}^3 \text{ molecule}^{-1} \text{ s}^{-1}$ in 700 Torr of N_2 . Smog chamber Fourier transform infrared (FTIR) techniques indicated that the acyl-forming channel accounts for $42 \pm 3\%$ of the reaction. The results are discussed with respect to the literature data and the importance of long range (greater than or equal to two carbon atoms along the aliphatic chain) effects in determining the reactivity of organic molecules toward chlorine atoms.

1. Introduction

Aldehydes (RCHO) are important trace constituents of the atmosphere. They have natural and anthropogenic sources, with small primary sources associated with vehicle exhaust and industrial activity and large secondary sources associated with the oxidation of volatile organic compounds.^{1,2} Abstraction of the aldehydic H atom by OH radicals gives acyl radicals, $\text{RC}(\text{O})$, that combine with O_2 to give acylperoxy radicals, $\text{RC}(\text{O})\text{O}_2$. Acylperoxy radicals have several important roles in atmospheric chemistry. $\text{RC}(\text{O})\text{O}_2$ radicals react rapidly with NO to give NO_2 , which is then photolyzed, leading to ozone formation. $\text{RC}(\text{O})\text{O}_2$ radicals react with NO_2 to form stable peroxyacylnitrates, $\text{RC}(\text{O})\text{O}_2\text{NO}_2$. Peroxyacylnitrates are severe, irritant compounds in photochemical smog, efficient reservoirs of NO_x in the troposphere, and they transport NO_x far from its sources.³ In air masses with low $[\text{NO}_x]$, acylperoxy radicals undergo reactions with HO_2 and other peroxy radicals. Reactions of $\text{RC}(\text{O})\text{O}_2$ with HO_2 radicals are important radical chain termination reactions and are a source of carboxylic acids in the atmosphere.

The kinetic database for atmospherically relevant reactions of acylperoxy radicals is limited. Acetaldehyde (ethanal) is often used as the model for the reactivity of aldehydes in chemical modeling of atmospheric chemistry. Data for larger acylperoxy radicals are needed for a more complete understanding of

atmospheric chemistry. Prior to a study of the atmospheric chemistry of $\text{CH}_3(\text{CH}_2)_3\text{C}(\text{O})\text{O}_2$ radicals, it is first necessary to characterize a suitable laboratory source for these radicals. The reaction of chlorine atoms with *n*-pentanal is a possible source of $\text{CH}_3(\text{CH}_2)_3\text{C}(\text{O})\text{O}_2$ radicals for laboratory experiments. To design and interpret such experiments accurate kinetic and mechanistic data concerning reaction 1



are needed. To fulfill this need, we report here a study of the kinetics and mechanism of the reaction of chlorine atoms with *n*-pentanal.

2. Experimental Section

2.1. PLP–LIF Measurement of $k[\text{Cl} + \text{CH}_3(\text{CH}_2)_3\text{CHO}]$ at Nagoya University. Absolute rate measurements of $k[\text{Cl} + \text{CH}_3(\text{CH}_2)_3\text{CHO}]$ were carried out using pulsed laser photolysis–vacuum ultraviolet laser-induced fluorescence (PLP–LIF) spectroscopy at Nagoya University. The experimental setup is described in detail elsewhere.⁴

Cl atoms were produced by the photolysis of Cl_2 [$(3.6 \times 10^{12}) - (1.1 \times 10^{13}) \text{ cm}^{-3}$] at 351 nm using a XeF excimer laser (Lambda Physik, COMPex 102). On the basis of the Cl_2 absorption cross section at 351 nm⁵ and the photolysis laser fluence [$(2.0 - 2.7) \times 10^{16} \text{ photons cm}^{-2}$], the initial $\text{Cl}(^2\text{P}_j)$ atom concentration was estimated to be in the range $(1.3 - 5.7) \times 10^{10}$

* Corresponding author. E-mail: twalling@ford.com.

cm^{-3} . The $\text{Cl}(^2\text{P}_{3/2})$ atoms were detected directly by PLP–LIF using the $3\text{p}^5\ ^2\text{P}_{3/2} - 3\text{p}^44\text{s}\ ^2\text{P}_{3/2}$ transition at 134.72 nm. On the basis of the reported value of $[\text{Cl}^*(^2\text{P}_{1/2})]/[\text{Cl}(^2\text{P}_{3/2})] = 0.016 \pm 0.001$ at 355 nm,⁶ it is expected that photolysis of Cl_2 at 351 nm will not generate significant amounts of electronically excited $\text{Cl}^*(^2\text{P}_{1/2})$ atoms. Consistent with this expectation, in a recent study⁴ we observed that the LIF intensity of $\text{Cl}^*(^2\text{P}_{1/2})$ at 135.17 nm corresponding to the $3\text{p}^5\ ^2\text{P}_{1/2} - 3\text{p}^44\text{s}\ ^2\text{P}_{1/2}$ transition was negligibly small compared with that of $\text{Cl}(^2\text{P}_{3/2})$ at 134.72 nm. We conclude that physical quenching and/or chemical reaction of $\text{Cl}^*(^2\text{P}_{1/2})$ does not interfere with our kinetic measurements.

Tunable VUV radiation around 135 nm was generated by two-photon resonant four-wave difference frequency mixing ($\omega_{\text{vuv}} = 2\omega_1 - \omega_2$) in Kr gas, using two tunable dye lasers (Lambda Physik, FL3002 and Scanmate 2E) pumped by a single XeCl excimer laser (Lambda Physik, COMPex 201). The typical pressure of Kr gas was 35 Torr. The $\text{Cl}(^2\text{P}_{3/2})$ LIF signal was detected by a solar-blind photomultiplier tube (EMR, 541J-08-17) with a KBr photocathode sensitive at 106–150 nm. The PMT tube was mounted at right angles to the propagation direction of the VUV probe beam and the 351 nm photolysis beam. The 351 nm laser light and the vacuum UV laser light crossed perpendicularly in the reaction cell. The pump and probe lasers were operated at a repetition rate of 10 Hz. The time delay between the dissociation and probe laser pulses was controlled by a pulse generator (Stanford Research, DG535), and the jitter of the delay time was less than 20 ns. The reaction chamber was evacuated continuously using a rotary pump (Edwards, RV-12) through a liquid nitrogen trap. Total pressure in the chamber was monitored using a capacitance manometer (MKS Baratron, Model 626IITAE).

The Cl atoms produced from photodissociation of Cl_2 at 351 nm have a nascent kinetic energy of 12.1 kcal mol⁻¹ in the laboratory frame. To thermalize the translationally hot Cl atoms, 8 Torr of Ar diluent was added to the reaction mixtures. Doppler profiles of the Cl atoms as a function of delay time were recorded by scanning the VUV laser wavelength to ensure that complete thermalization of the translational energy of Cl atoms was achieved before their reaction with the $\text{CH}_3(\text{CH}_2)_3\text{CHO}$. The Doppler shifts reflect the velocity components of the Cl fragments along the propagation direction of the probe laser beam.⁷ We observed that the translational energy distribution of Cl atoms was thermalized by collisions with Ar within 5 μs . Kinetic data were acquired by fitting the Cl atom decay traces at times $>5\ \mu\text{s}$.

The gas mixtures of 0.11–0.34 mTorr of Cl_2 and 0.99–19 mTorr of $\text{CH}_3(\text{CH}_2)_3\text{CHO}$ in Ar diluent were slowly introduced into the reaction chamber through mass flow controllers (Horiba STEC, SEC-400MARK3). The reactant concentrations in the chamber were estimated using the mass flow rates and pressures. Reagents diluted with Ar were stored in 10-L glass bulbs that were blackened to avoid any photochemistry. Reagents of Cl_2 (Sumitomo Seika Co., >99%), $\text{CH}_3(\text{CH}_2)_3\text{CHO}$ (Wako Chemicals, >98.0%), and Ar (Nihon Sanso, >99.999%) were used without further purification. All experiments were performed at $295 \pm 2\ \text{K}$.

2.2. Relative Rate Experiments at the University of Michigan–Dearborn. Relative rate experiments were carried out in a spherical, Pyrex (500 cm³) reactor interfaced to a gas chromatograph (HP 5890 GC/FID with a 30 m, 320 μm , DB-1 capillary column with 5 μm coating) at the University of Michigan–Dearborn. Experiments were performed using Cl_2/n -pentanal/ $\text{C}_3\text{H}_8/\text{CH}_4$ mixtures in N_2 (UHP) or air diluents (Cl_2

and pentanal purities >99.7% and 97%, respectively; freeze/thaw cycles were performed on the n -pentanal and Cl_2 reactants). Methane (research grade, 99.997%) and C_3H_8 (research grade, 99.97%) were used as supplied. Methane was used for internal calibration of the GC analysis, since it is essentially unreactive toward Cl ($k = 1 \times 10^{-13}\ \text{cm}^3\ \text{molecule}^{-1}\ \text{s}^{-1}$)⁵ relative to the other hydrocarbons in the mixture. Propane was used as the reference compound in the GC relative rate experiments because it is convenient to measure using the GC technique and because k_2 is well-established and independent of pressure.



Each reactant sample was mixed in the reactor prior to irradiation. Chlorine atoms were generated by irradiation with UV light using a single Sylvania F6T5 BLB fluorescent lamp. The reactor was rotated slowly during the irradiation to achieve more uniform illumination of the reactant mixture.



After a chosen irradiation time, a portion of the contents of the reactor was removed (either from the flask through a gas handling system into the GC sample loop or indirectly using a 1 cm³ gastight syringe to transfer the sample directly into the GC injector port) and analyzed by gas chromatography. The different injection techniques gave results that were indistinguishable within the experimental uncertainties. The mixture was then irradiated for additional times, and additional analyses were performed. The relative rate method is a well-established technique for measuring the reactivity of Cl atoms with organic compounds.⁸ Kinetic data are derived by monitoring the loss of pentanal and the reference compound (C_3H_8 in the present study). The decays of pentanal and C_3H_8 are then plotted using the expression

$$\ln\left(\frac{[\text{pentanal}]_{t_0}}{[\text{pentanal}]_t}\right) = \frac{k_1}{k_2} \ln\left(\frac{[\text{C}_3\text{H}_8]_{t_0}}{[\text{C}_3\text{H}_8]_t}\right)$$

where $[\text{pentanal}]_{t_0}$, $[\text{pentanal}]_t$, $[\text{C}_3\text{H}_8]_{t_0}$, and $[\text{C}_3\text{H}_8]_t$ are the concentrations of pentanal and C_3H_8 at times “ t_0 ” and “ t ”, k_1 and k_2 are the rate constants for reactions of Cl atoms with the pentanal and C_3H_8 . Plots of $\ln([\text{pentanal}]_{t_0}/[\text{pentanal}]_t)$ versus $\ln([\text{C}_3\text{H}_8]_{t_0}/[\text{C}_3\text{H}_8]_t)$ should be linear, pass through the origin, and have a slope of k_1/k_2 .

Initial reagent concentrations in 800–950 Torr of N_2 diluent were 55–180 mTorr of n -pentanal, 8–275 mTorr of C_3H_8 , 100–300 mTorr of CH_4 , and 140–950 mTorr of Cl_2 . In 800–950 Torr of air, the initial concentrations were 130–190 mTorr of n -pentanal, 19–28 mTorr of C_3H_8 , 230–300 mTorr of CH_4 , and 225–1200 mTorr of Cl_2 . On the basis of the irradiation times (2–30 s in N_2 and 40–600 s in air), pentanal consumption, and the value of k_1 , the estimated range of steady-state Cl atom concentrations were $(2-20) \times 10^8\ \text{cm}^{-3}$ in N_2 and $(1-7) \times 10^7$ in air diluent. In relative rate experiments it is important to check for unwanted loss of reactants and references via photolysis, dark chemistry, and heterogeneous reactions. There was no observable loss of n -pentanal upon irradiation of mixtures in N_2 for 3 min in the absence of Cl_2 . Control experiments were performed in which mixtures both before and after the UV irradiation of reactant mixtures were allowed to stand in the dark in the reactor for 20–30 min. There was no observable loss of the reactant or reference. Unless stated otherwise, quoted uncertainties in the rate constant ratios are two standard deviations from least-squares regressions.

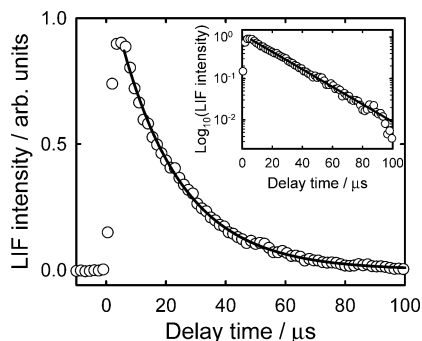


Figure 1. A typical $\text{Cl}(^2\text{P}_{3/2})$ decay profile observed in an experiment using a mixture of 0.3 mTorr of Cl_2 and 6.1 mTorr of $\text{CH}_3(\text{CH}_2)_3\text{CHO}$ in 8.0 Torr of Ar diluent at 295 ± 2 K. The insert shows a semilogarithmic plot of the temporal decay of the VUV–LIF signal of $\text{Cl}(^2\text{P}_{3/2})$ atoms. The initial jump in the profile reflects the photolytic formation of $\text{Cl}(^2\text{P}_{3/2})$ atoms from Cl_2 at 351 nm. The lines through the data are least-squares fits assuming first-order kinetics.

2.3. Smog Chamber Experiments at Ford. The smog chamber system at Ford Motor Co. consists of a 140 L Pyrex reactor interfaced to a Mattson Sirius 100 spectrometer.⁹ The reactor was surrounded by 22 fluorescent blacklamps (GE F15T8-BL). Relative rate techniques were used to measure the reactivity of chlorine atoms toward $\text{CH}_3(\text{CH}_2)_3\text{C}(\text{O})\text{Cl}$. Chlorine atoms were generated by photolysis of molecular chlorine in 700 Torr of air diluent at 295 ± 2 K.

The loss of the reactant and reference compounds was monitored by FTIR spectroscopy using an infrared path length of 27 m and a resolution of 0.25 cm^{-1} . Infrared spectra were derived from 32 coadded interferograms. Analysis of the IR spectra was achieved through spectral stripping, in which small fractions of the reference spectrum were subtracted incrementally from the sample spectrum. The concentrations of reactant and reference compounds were determined with a precision of $\pm 1\%$ of their initial concentrations. Reagents were obtained from commercial sources at $>99\%$ purity and were subjected to repeated freeze/pump/thaw cycling before use. Ultra-high-purity air was used as the diluent gas.

In smog chamber experiments, it is important to check for unwanted loss of reactants and products via photolysis, dark chemistry, and heterogeneous reactions. Control experiments were performed in which (i) mixtures of reactants (except Cl_2) were subjected to UV irradiation for 10–20 min and (ii) product mixtures obtained after the UV irradiation of reactant mixtures were allowed to stand in the dark in the chamber for 20 min. There was no observable loss of reactants or products, suggesting that photolysis, dark chemistry, and heterogeneous reactions are not significant complications in the present work. Unless stated otherwise, quoted uncertainties are two standard deviations from least-squares regressions.

3. Results

3.1. PLP–LIF Study of $k[\text{Cl} + \text{CH}_3(\text{CH}_2)_3\text{CHO}]$ at Nagoya University. Figure 1 shows a trace of the observed temporal profile of the $\text{Cl}(^2\text{P}_{3/2})$ LIF signal following the 351 nm pulsed laser irradiation of a mixture of 0.3 mTorr of Cl_2 and 6.1 mTorr of $\text{CH}_3(\text{CH}_2)_3\text{CHO}$ in 8.0 Torr of Ar diluent. The time-resolved $\text{Cl}(^2\text{P}_{3/2})$ LIF signal produced by the 351 nm pulsed laser photolysis of Cl_2 exhibits an initial jump followed by a slowly decay, which is attributed predominately to chemical loss of Cl atoms (loss via diffusion from the viewing zone makes a minor contribution). As seen from Figure 1, the semilogarithmic

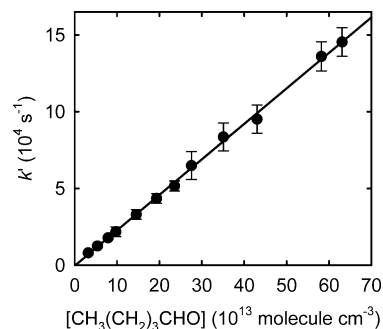


Figure 2. Pseudo-first-order loss of $\text{Cl}(^2\text{P}_{3/2})$ atoms versus $[\text{CH}_3(\text{CH}_2)_3\text{CHO}]$. The line through the data is a linear least-squares fit.

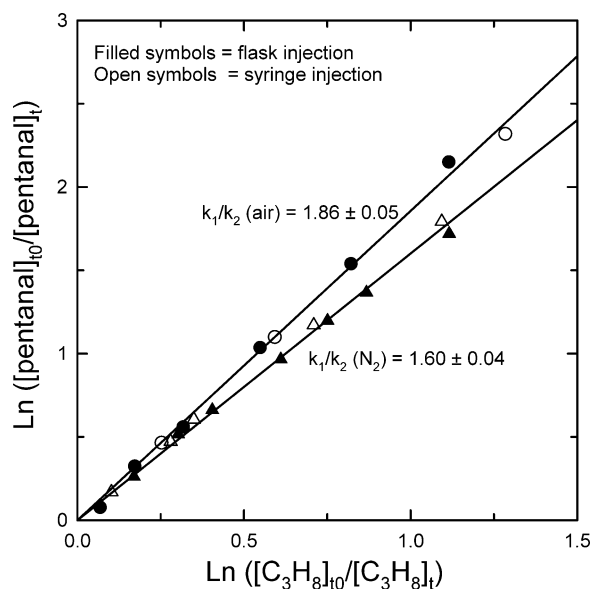


Figure 3. Loss of $\text{CH}_3(\text{CH}_2)_3\text{CHO}$ versus C_3H_8 following exposure to Cl atoms in 800–950 Torr of N_2 (triangles) or air (circles) at 296 K. Filled and open symbols were obtained using flask or syringe sampling techniques, respectively. The rate constant ratios are least-squares fits to the data with 2σ error limits.

plots of the $\text{Cl}(^2\text{P}_{3/2})$ LIF signal indicate that the Cl atoms are consumed by a pseudo-first-order decay process at delay times $> 5 \mu\text{s}$.

The pseudo-first-order rate constants, k' , obtained from the decay profiles such as that shown in Figure 1 are plotted versus $\text{CH}_3(\text{CH}_2)_3\text{CHO}$ concentrations in Figure 2. Linear least-squares fit analysis of the data in Figure 2 gives $k[\text{Cl} + \text{CH}_3(\text{CH}_2)_3\text{CHO}] = (2.31 \pm 0.35) \times 10^{-10} \text{ cm}^3 \text{ molecule}^{-1} \text{ s}^{-1}$. Quoted uncertainties include two standard deviations from the linear regression analysis and our estimate of systematic uncertainties, such as the accuracy of the concentration measurements.

3.2. Relative Rate Study of $k[\text{Cl} + \text{CH}_3(\text{CH}_2)_3\text{CHO}]$ at the University of Michigan–Dearborn. Figure 3 shows the loss of pentanal relative to the reference compound, propane, in both air (circle symbol) and nitrogen (triangle symbol) diluents. As discussed in section 2.2, the slope of the least-squares fits to these two data sets provides the rate constant ratio k_1/k_2 in each diluent. The two sampling techniques used (see section 2.2) gave identical rate constant ratios to within experimental error as shown in Figure 3.

In N_2 diluent, the measured rate constant ratio k_1/k_2 is 1.60 ± 0.04 . The error limit represents two standard deviations from the least-squares fit to the data points in Figure 3. When combined with $k_2 = (1.4 \pm 0.1) \times 10^{-10} \text{ cm}^3 \text{ molecule}^{-1} \text{ s}^{-1}$,⁵ the resulting value of k_1 is $(2.24 \pm 0.20) \times 10^{-10} \text{ cm}^3$

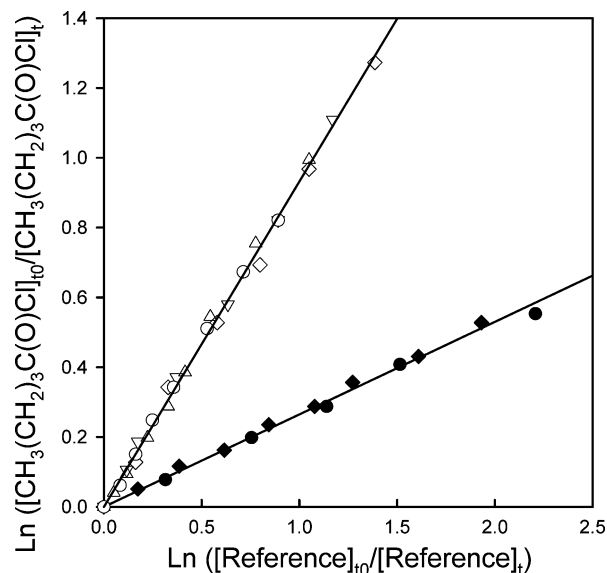
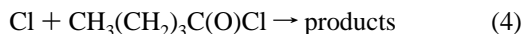


Figure 4. Loss of $\text{CH}_3(\text{CH}_2)_3\text{C}(\text{O})\text{Cl}$ versus C_2H_4 (open symbols) and C_6H_{12} (closed symbols) following exposure to Cl atoms in 700 Torr of air at 295 K. Different symbols represent separate experiments.

molecule⁻¹ s⁻¹. In the presence of air, the rate constant ratio $k_1/k_2 = 1.86 \pm 0.05$ is slightly, but significantly, larger than in N_2 . It has been reported recently that the reaction of $\text{CH}_3\text{C}(\text{O})\text{O}_2$ with HO_2 radicals gives OH radicals in a yield of approximately 40%.^{10,11} For experiments conducted in air, both $\text{CH}_3(\text{CH}_2)_3\text{C}(\text{O})\text{O}_2$ and HO_2 radicals will be present, and it seems reasonable to expect that OH radicals will be generated in the system. Pentanal reacts with OH at a much faster rate ($2.8 \times 10^{-11} \text{ cm}^3 \text{ molecule}^{-1} \text{ s}^{-1}$)¹² than does propane (1.1×10^{-12}),⁵ and the formation of OH radicals will lead to an overestimation of k_1/k_2 consistent with our measurement of $k_1/k_2 = 1.60 \pm 0.04$ in N_2 diluent and $k_1/k_2 = 1.86 \pm 0.05$ in air diluent. While this effect is relatively small, it should be considered in future relative rate studies where aldehydes are present.

3.3. Relative Rate Study of $k[\text{Cl} + \text{CH}_3(\text{CH}_2)_3\text{C}(\text{O})\text{Cl}]$ at Ford. The rate of reaction 4 was measured relative to reactions 5 and 6:



Reaction mixtures consisted of 7.6–29.9 mTorr of $\text{CH}_3(\text{CH}_2)_3\text{C}(\text{O})\text{Cl}$, 100 mTorr of Cl_2 , and either 3.2 mTorr of C_2H_4 or 3.2–4.6 mTorr of C_6H_{12} , in 700 Torr of air diluent. Figure 4 shows the loss of $\text{CH}_3(\text{CH}_2)_3\text{C}(\text{O})\text{Cl}$ versus loss of the reference compounds following the UV irradiation of $\text{CH}_3(\text{CH}_2)_3\text{C}(\text{O})\text{Cl}/\text{Cl}_2/\text{reference}/\text{air}$ mixtures. Linear least-squares analysis of the data in Figure 4 gives $k_4/k_5 = 0.93 \pm 0.09$ and $k_4/k_6 = 0.26 \pm 0.03$. The quoted uncertainties include two standard deviations from the linear regression analyses and our estimate of uncertainties in the spectral analysis.

Using $k_5 = (9.29 \pm 0.51) \times 10^{-11}$ ¹³ and $k_6 = (3.4 \pm 0.3) \times 10^{-10}$,¹⁴ we derive $k_4 = (8.64 \pm 0.96) \times 10^{-11}$ and $(8.84 \pm 1.28) \times 10^{-11} \text{ cm}^3 \text{ molecule}^{-1} \text{ s}^{-1}$. Consistent results were obtained in experiments conducted using the two different reference compounds. We choose to cite a final value that is the average together with error limits which encompass the extremes of the individual determinations, $k_4 = (8.74 \pm 1.38)$

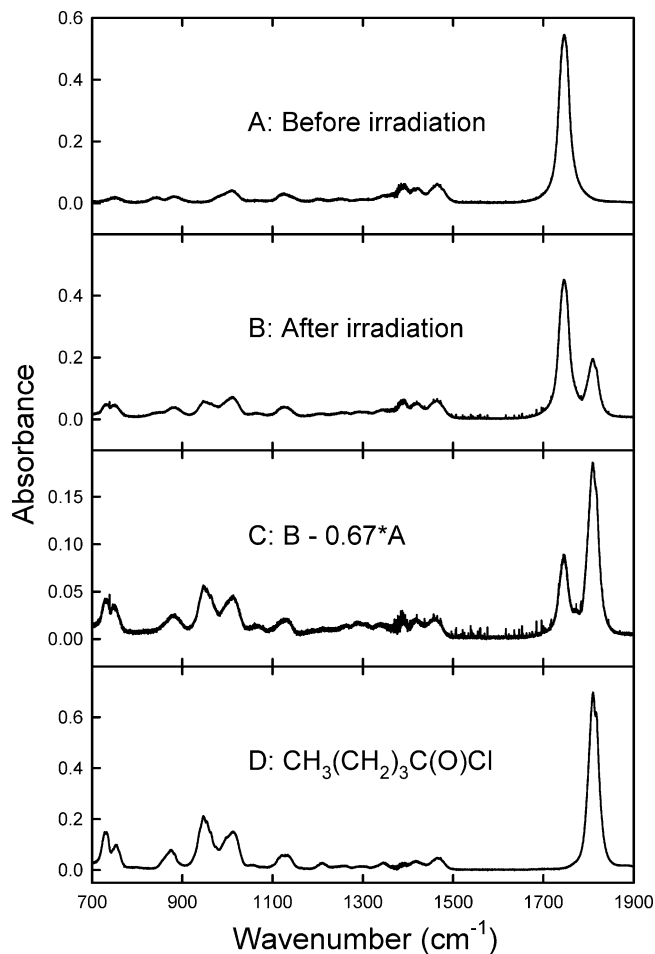


Figure 5. IR spectra before (A) and after (B) a 9 s irradiation of a mixture of 23.4 mTorr of $\text{CH}_3(\text{CH}_2)_3\text{CHO}$ and 100 mTorr of Cl_2 in 700 Torr of N_2 at 295 K. The consumption of $\text{CH}_3(\text{CH}_2)_3\text{CHO}$ was 33%. Spectrum C shows the results of subtracting $\text{CH}_3(\text{CH}_2)_3\text{CHO}$ features from spectrum B. Panel D is a reference spectrum of $\text{CH}_3(\text{CH}_2)_3\text{C}(\text{O})\text{Cl}$.

$\times 10^{-11} \text{ cm}^3 \text{ molecule}^{-1} \text{ s}^{-1}$. Comparing this result to $k[\text{Cl} + \text{CH}_3(\text{CH}_2)_3\text{CHO}] = 2.3 \times 10^{-10} \text{ cm}^3 \text{ molecule}^{-1} \text{ s}^{-1}$, we conclude that substitution of the aldehydic hydrogen by a Cl atom reduces the reactivity of the molecule by a factor of approximately 2.6.

3.4. Mechanistic Study of the $\text{Cl} + \text{CH}_3(\text{CH}_2)_3\text{CHO}$ Reaction at Ford. To provide information on the mechanism of the reaction of Cl atoms with $\text{CH}_3(\text{CH}_2)_3\text{CHO}$, experiments were performed in which mixtures of 21.2–27.5 mTorr of $\text{CH}_3(\text{CH}_2)_3\text{CHO}$ and 100–1000 mTorr of Cl_2 in 700 Torr of N_2 diluent were subjected to UV irradiation. Figure 5 shows typical IR spectra obtained before and after 9 s of UV irradiation of 23.4 mTorr of $\text{CH}_3(\text{CH}_2)_3\text{CHO}$ and 100 mTorr of Cl_2 in 700 Torr of N_2 diluent. Panel C in Figure 5 shows the result of subtracting features that are attributable to $\text{CH}_3(\text{CH}_2)_3\text{CHO}$ (using its feature at 2713 cm^{-1}) from panel B. It should be noted that the fact that a carbonyl feature still remains at 1746 cm^{-1} in panel C does not reflect an inadequate subtraction of *n*-pentanal features. The subtraction of IR features attributable to *n*-pentanal was achieved using its characteristic features at 2713 and, to a lesser extent, 842 cm^{-1} . The residual carbonyl feature at 1746 cm^{-1} in panel C presumably reflects the formation of 2-, 3-, 4-, and 5-chloropentanal in the system. A reference spectrum of $\text{CH}_3(\text{CH}_2)_3\text{C}(\text{O})\text{Cl}$ is given in panel D. It is clear from an inspection of Figure 5 that $\text{CH}_3(\text{CH}_2)_3\text{C}(\text{O})\text{Cl}$ is a major product.

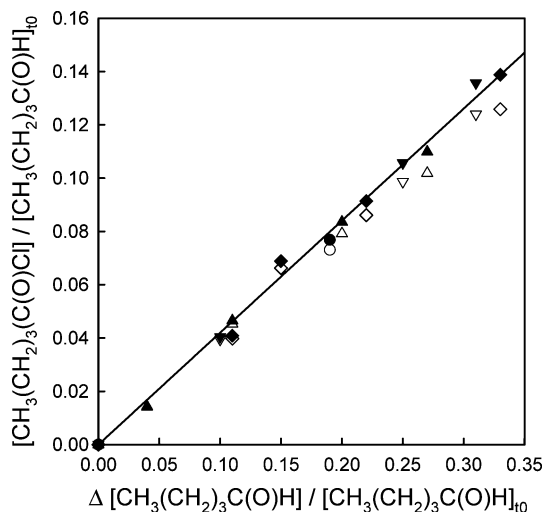


Figure 6. Formation of $\text{CH}_3(\text{CH}_2)_3\text{C}(\text{O})\text{Cl}$ versus loss of $\text{CH}_3(\text{CH}_2)_3\text{CHO}$, following UV irradiation mixtures of 21.2 mTorr $\text{CH}_3(\text{CH}_2)_3\text{CHO}$ and 100 mTorr Cl_2 (circles), 23.4 mTorr $\text{CH}_3(\text{CH}_2)_3\text{CHO}$ and 100 mTorr Cl_2 (diamonds), 27.4 mTorr $\text{CH}_3(\text{CH}_2)_3\text{CHO}$ and 100 mTorr Cl_2 (triangles), and 27.5 mTorr $\text{CH}_3(\text{CH}_2)_3\text{CHO}$ and 1000 mTorr Cl_2 (inverted triangles) in 700 Torr of N_2 at 296 K. Filled symbols have been corrected for secondary loss of $\text{CH}_3(\text{CH}_2)_3\text{C}(\text{O})\text{Cl}$; see the text for details.

$\text{CH}_3(\text{CH}_2)_3\text{C}(\text{O})\text{Cl}$ is produced by reactions 1a and 7 and provides a measure of the importance of reaction channel 1a.



As shown in section 3.3, $\text{CH}_3(\text{CH}_2)_3\text{C}(\text{O})\text{Cl}$ reacts with chlorine atoms. The concentration profile of a reactive primary product such as $\text{CH}_3(\text{CH}_2)_3\text{C}(\text{O})\text{Cl}$ is described¹⁵ by the following expression:

$$\frac{[\text{CH}_3(\text{CH}_2)_3\text{C}(\text{O})\text{Cl}]_t}{[\text{CH}_3(\text{CH}_2)_3\text{CHO}]_{t_0}} = \left\{ \frac{\alpha}{(1 - (k_4/k_1))} \right\} (1 - x) \{ (1 - x)^{(k_4/k_1) - 1} - 1 \}$$

where $x = 1 - ([\text{CH}_3(\text{CH}_2)_3\text{CHO}]_t / [\text{CH}_3(\text{CH}_2)_3\text{CHO}]_{t_0})$ (the fractional consumption of $\text{CH}_3(\text{CH}_2)_3\text{CHO}$ at time t) and α is the yield of $\text{CH}_3(\text{CH}_2)_3\text{C}(\text{O})\text{Cl}$ following reaction of Cl with $\text{CH}_3(\text{CH}_2)_3\text{CHO}$. The loss of $\text{CH}_3(\text{CH}_2)_3\text{C}(\text{O})\text{Cl}$ via reaction with Cl atoms can be corrected for using the expression above. Figure 6 shows a plot of $[\text{CH}_3(\text{CH}_2)_3\text{C}(\text{O})\text{Cl}] / [\text{CH}_3(\text{CH}_2)_3\text{CHO}]_{t_0}$ versus $[\text{CH}_3(\text{CH}_2)_3\text{CHO}] / [\text{CH}_3(\text{CH}_2)_3\text{CHO}]_{t_0}$; open symbols are the observed data, and filled symbols have been corrected for loss via reaction with Cl atoms. As seen from Figure 6, variation of $[\text{Cl}_2]$ by a factor of 10 had no observable impact on the results, leading us to conclude that essentially all of the $\text{CH}_3(\text{CH}_2)_3\text{C}(\text{O})$ radicals formed in the system are scavenged by reaction with Cl_2 . The line through the corrected data in Figure 6 is a linear least-squares fit that gives a molar $\text{CH}_3(\text{CH}_2)_3\text{C}(\text{O})\text{Cl}$ yield of 0.42 ± 0.03 . We conclude that abstraction of the aldehydic hydrogen accounts for $42 \pm 3\%$ of the reaction of Cl atoms with $\text{CH}_3(\text{CH}_2)_3\text{CHO}$.

4. Discussion

4.1. Kinetics of the Cl + $\text{CH}_3(\text{CH}_2)_3\text{CHO}$ Reaction. The kinetics of the title reaction were studied using an absolute

TABLE 1: Literature Values of $k[\text{Cl} + \text{CH}_3(\text{CH}_2)_3\text{CHO}]$

rate coefficient ^a	temp (K)	total pressure ^b	diluent	expl technique ^c	reference
$(2.31 \pm 0.35) \times 10^{-10}$	295	8	Ar	PLP-LIF	this work
$(2.24 \pm 0.20) \times 10^{-10}$	296	800–950	N_2	RR	this work
$(2.6 \pm 0.3) \times 10^{-10}$	298	800–950	He	RR	16
$(2.56 \pm 0.27) \times 10^{-10}$	298	760	N_2 , air	RR	17
$(1.89 \pm 0.24) \times 10^{-10}$	298	20–200	He	PLP-RF	18

^a Units of $\text{cm}^3 \text{ molecule}^{-1} \text{ s}^{-1}$. ^b Units of Torr. ^c RR, relative rate; PLP-RF, pulsed laser photolysis–resonance fluorescence; PLP-LIF, pulsed laser photolysis–vacuum ultraviolet laser-induced fluorescence spectroscopy.

technique in 8 Torr of argon and a relative rate technique in 800–950 Torr of N_2 . The absolute rate study gave $k_1 = (2.31 \pm 0.35) \times 10^{-10}$, while the relative rate study gave $k_1 = (2.24 \pm 0.20) \times 10^{-10} \text{ cm}^3 \text{ molecule}^{-1} \text{ s}^{-1}$. The reaction is expected to proceed via hydrogen atom abstraction and hence its rate is not expected to show a dependence on total pressure. Consistent with expectations, the results from our absolute rate study at low pressure and the relative rate study at high pressure were indistinguishable.

The results from the present work are compared to the literature data in Table 1. Our results for $k[\text{Cl} + \text{CH}_3(\text{CH}_2)_3\text{CHO}]$ are in agreement with those from previous relative rate studies by Thévenet et al.¹⁶ and Rodríguez et al.¹⁷ However, our results are approximately 20% greater than that reported in the absolute rate study by Cuevas et al.,¹⁸ although the results from the two studies overlap within the combined experimental uncertainties. A possible explanation for this modest discrepancy lies in the experimental conditions used by Cuevas et al.¹⁸

In the pulsed laser photolysis–resonance fluorescence (PLP–RF) experiments by Cuevas et al.,¹⁸ kinetic data were obtained by monitoring the decay of Cl atoms in the presence of $\text{CH}_3(\text{CH}_2)_3\text{CHO}$. As in the present study, Cuevas et al. used the photolysis of Cl_2 as the source of chlorine atoms. As noted previously,^{18,19} alkyl radicals formed in reaction 1 will react with Cl_2 to regenerate Cl atoms, leading to a decrease in the measured rate of Cl atom decay and underestimation of k_1 . To minimize this problem Cuevas et al. added O_2 to the system to scavenge the alkyl radicals, however the amount of O_2 that could be added was limited by two complications, leading to signal attenuation: (i) O_2 absorbs the vacuum UV from the lamp and subsequent fluorescence from the Cl atoms, and (ii) O_2 quenches the Cl atom fluorescence signal. To avoid these complications, we used $[\text{CH}_3(\text{CH}_2)_3\text{CHO}] / [\text{Cl}_2]$ ratios that were approximately 100 times greater than those used by Cuevas et al. As a consequence, in the present study the time scale for Cl atom regeneration is decoupled from that of the experimental observations. In the study by Cuevas et al., the time scales were comparable. While the addition of O_2 by Cuevas et al. removed most of the complications caused by regeneration of Cl atoms, it did not eliminate Cl atom regeneration entirely, and this probably led to a modest underestimation of k_1 . It is interesting to note that, for each of the five compounds studied by Cuevas et al., the rate constants reported are lower than in all previous studies (see Table 3 in Cuevas et al.¹⁸). We suggest there is probably a small (approximately 10–20%) systematic underestimation of $k[\text{Cl} + \text{RCHO}]$ in the study by Cuevas et al.¹⁸

4.2. Mechanism of the Cl + $\text{CH}_3(\text{CH}_2)_3\text{CHO}$ Reaction. From the observed formation of $\text{CH}_3(\text{CH}_2)_3\text{C}(\text{O})\text{Cl}$, we conclude that $42 \pm 3\%$ of the reaction of Cl atoms proceeds via abstraction of the aldehydic hydrogen atom. Reference spectra for 2-, 3-, 4-, and 5-chloropentanal are not available, and we are not able to provide any information concerning the relative

importance of hydrogen abstraction in the rest of the pentanal molecule. Combining $k_{1a}/k_1 = 0.42 \pm 0.03$ with $k_1 = (2.31 \pm 0.35) \times 10^{-10}$ gives a site specific rate constant of $k_{1a} = (9.7 \pm 1.6) \times 10^{-11} \text{ cm}^3 \text{ molecule}^{-1} \text{ s}^{-1}$. This result can be compared to the rate constants for aldehydic hydrogen abstraction from ethanal and propanal of 7.6×10^{-11} ²⁰ and $(10.6 \pm 2.1) \times 10^{-11} \text{ cm}^3 \text{ molecule}^{-1} \text{ s}^{-1}$,²¹ respectively. For aldehydes with the general formula $\text{CH}_3(\text{CH}_2)_n\text{CHO}$, there is no discernible effect of molecular size on the rate of abstraction of the aldehydic hydrogen.

The reactivity of the $\text{CH}_3(\text{CH}_2)_3-$ group in pentanal, $k_1 - k_{1a} = 1.34 \times 10^{-10}$, and in pentanoyl chloride, $k_4 = (8.74 \pm 1.38) \times 10^{-11}$, can be compared to the reactivity of the same group in *n*-octane, $2.03 \times 10^{-10} \text{ cm}^3 \text{ molecule}^{-1} \text{ s}^{-1}$.⁸ The $-\text{CHO}$ group in *n*-pentanal and the $-\text{C}(\text{O})\text{Cl}$ group in pentanoyl chloride have a significant deactivating effect on the rest of the molecule. The reactivity of the $\text{CH}_3(\text{CH}_2)_2-$ group in *n*-hexane is $1.50 \times 10^{-10} \text{ cm}^3 \text{ molecule}^{-1} \text{ s}^{-1}$.⁸ From the fact that the reactivity of the $\text{CH}_3(\text{CH}_2)_3-$ groups in *n*-pentanal and pentanoyl chloride are less than that of the one carbon atom smaller $\text{CH}_3(\text{CH}_2)_2-$ group in *n*-hexane, it can be concluded that the deactivating effect of the $-\text{CHO}$ and $-\text{C}(\text{O})\text{Cl}$ groups extend over at least two carbons in the aliphatic chain. Such long-range effects complicate the development of simple structure–activity relationship (SAR) approaches to estimate the reactivity of organic molecules toward chlorine atoms which typically consider only nearest neighbor effects.⁸ As the chlorine atom kinetic database increases in both scope and quality, in the future it will be possible to include long-range effects, which should improve the ability of SARs to predict the reactivity of organic compounds for which no experimental data are available. The kinetic and mechanistic data presented herein will facilitate the design and interpretation of laboratory experiments of the atmospheric chemistry of $\text{CH}_3(\text{CH}_2)_3\text{C}(\text{O})\text{O}_2$ radicals.

Acknowledgment. The Nagoya group thanks Grant-in-Aid from the Ministry of Education, Culture, Sports, Science, and Technology, Japan. E.W.K. thanks Prof. Craig Donahue for invaluable assistance during the experiments at University of Michigan–Dearborn. This study was partly supported by the

Program for Improvement of Research Environment for Young Researchers from Special Coordination Funds for Promoting Science and Technology (SCF) commissioned by the MEXT of Japan.

References and Notes

- (1) Satsumabayashi, H.; Kurita, H.; Chang, Y. S.; Carmichael, G. R.; Ueda, H. *Atmos. Environ.* **1995**, *29*, 255.
- (2) Viskari, E. L.; Vartiainen, M.; Pasanen, P. *Atmos. Environ.* **2000**, *34*, 917.
- (3) Beine, H. J.; Jaffe, D. A.; Hering, J. A.; Kelley, J. A.; Krognes, T.; Stordal, F. *J. Atmos. Chem.* **1997**, *27*, 127.
- (4) Takahashi, K.; Iwasaki, E.; Matsumi, Y.; Wallington, T. J. *J. Phys. Chem. A* **2007**, *111*, 1271.
- (5) Sander, S. P.; Friedl, R. R.; Golden, D. M.; Kurylo, M. J.; Moortgat, G. K.; Keller-Rudek, H.; Wine, P. H.; Ravishankara, A. R.; Kolb, C. E.; Molina, M. J.; Finlayson-Pitts, B. J.; Huie, R. E.; Orkin, V. L. *Chemical Kinetics and Photochemical Data for Use in Atmospheric Studies*; Evaluation No. 15, JPL Publication 06-2, 2006.
- (6) Matsumi, Y.; Tonokura, K.; Kawasaki, M.; *J. Chem. Phys.* **1992**, *97*, 1065.
- (7) Zare, R. N.; Herschbach, D. R. *Proc. IEEE* **1963**, *51*, 173.
- (8) Aschmann, S. M.; Atkinson, R. *Int. J. Chem. Kinet.* **1995**, *27*, 613.
- (9) Wallington, T. J.; Japar, S. M. *J. Atmos. Chem.* **1989**, *9*, 399.
- (10) Hasson, A. S.; Tyndall, G. S.; Orlando, J. J. *J. Phys. Chem. A* **2004**, *108*, 5979.
- (11) Jenkin, M. E.; Hurley, M. D.; Wallington, T. J. *Phys. Chem. Chem. Phys.* **2007**, *9*, 3149.
- (12) Semmes, D. H.; Ravishankara, A. R.; Gump-Perkins, C. A.; Wine, P. H. *Int. J. Chem. Kinet.* **1985**, *17*, 303.
- (13) Wallington, T. J.; Andino, J. M.; Lorkovic, I. M.; Kaiser, E. W.; Marston, G. *J. Phys. Chem.* **1990**, *94*, 3644.
- (14) Wallington, T. J.; Guschin, A.; Hurley, M. D. *Int. J. Chem. Kinet.* **1998**, *30*, 310.
- (15) Meagher, R. J.; McIntosh, M. E.; Hurley, M. D.; Wallington, T. J. *Int. J. Chem. Kinet.* **1997**, *29*, 619.
- (16) Thévenet, R.; Mellouki, A.; Le Bras, G. *Int. J. Chem. Kinet.* **2000**, *32*, 676.
- (17) Rodríguez, D.; Rodríguez, A.; Notario, A.; Aranda, A.; Díaz de Mera, Y.; Martínez, E. *Atmos. Chem. Phys.* **2005**, *5*, 3433.
- (18) Cuevas, C. A.; Notario, A.; Martínez, E.; Albaladejo, J. *Atmos. Environ.* **2006**, *40*, 3845.
- (19) Taketani, F.; Matsumi, Y.; Wallington, T. J.; Hurley, M. D. *Chem. Phys. Lett.* **2006**, *431*, 257.
- (20) Niki, H.; Maker, P. D.; Savage, C. M.; Breitenbach, L. P. *J. Phys. Chem.* **1985**, *89*, 588.
- (21) Le Crâne, J.-P.; Villenave, E.; Hurley, M. D.; Wallington, T. J.; Ball, J. C. *J. Phys. Chem. A* **2005**, *109*, 11837.